

«««< HEAD ===== »»»> 6188fac044d2ea13f89e1169cada113c0d6ce733
«««< HEAD ===== »»»> 6188fac044d2ea13f89e1169cada113c0d6ce733
«««< HEAD ===== »»»> 6188fac044d2ea13f89e1169cada113c0d6ce733
«««< HEAD =====
»»»> 6188fac044d2ea13f89e1169cada113c0d6ce733

««< HEAD ===== »»> 6188fac044d2ea13f89e1169cada113c0d6ce733 ««<
HEAD ===== »»> 6188fac044d2ea13f89e1169cada113c0d6ce733 ««< HEAD =====
»»> 6188fac044d2ea13f89e1169cada113c0d6ce733 ««< HEAD ===== »»> 6188fac044d2ea13f89e1

Chapter 1

Future Work: Structure-Property in the PAL30 Homologous Series of Molecules

Now that the existance of the $\text{Sm}(\text{CP})_\alpha$ and $\text{SmC}_\text{A}\text{P}_\text{A}$ phase have been put on a firm footing, we can extend this study to a broad category of molecules that share the same core, but have variations in the tail length. Our previous study focussed on PAL30, with a tail length of $n=14$ carbons. Inspired by previous studies by the Dublin group[?, ?, ?], where the n_{16} and n_{18} compounds were studied and a helical phase was tentatively determined based on periodicities of around $5n$ seen in atomic force microscopy images. This is a test. With the ability to directly probe the periodicity of these compounds with carbon K-edge resonant X-ray, we have the ability to provide direct evidence for helical phases in these molecules. The high-resolution provided by RSoXS additionally allows for a rich study of structure-property relationships, where the nature of the helical phase can be connected to the tail-length.

Interest in the PAL30 series of molecules is not confined to the discovery of helicity. The additional discovery of a bent-core de Vries like phase is also a motivating interest for study of this series.

This chapter is organized under discussion of these two phases. First the helical, smectic $\text{Sm}(\text{CP})_\alpha$ is presented and discussed for the n_{12} , n_{14} , and n_{16} molecules. Then the bent-core de Vries phase is presented and discussed for this series.

1.1 The $\text{Sm}(\text{CP})_\alpha$ Phase: Smectic Chirality Beyond the B2 Phase

1.2 The bent-core de Vries phase

The evidence for a bent-core de Vries phase in PAL30 will be briefly reviewed. It is worth noting that the question of “what is a de Vries phase” is not settled, even for the simpler phases of rod-shaped molecules, see Jan Lagerwall’s thesis[?] for an excellent history and discussion of de Vries phases in the calamitic paradigm. For the purposes of this thesis, we take the broadest view of a de Vries: it is a tilted phase with no long-range order present in the tilt order parameter.

Even this broad definition is not free from ambiguity— what entails long-range order, and does it matter how the escape from long-range order is achieved? We will also see in this Chapter that the de Vries phase can be suppressed quite easily by a strong-alignment layer.

To satisfy our definition, we must prove two things about the phase under investigation to say it is a de Vries bent-core phase. First, it must be tilted. Second, it must have no long-range order present. Both of these facts are very difficult to establish in a positive manner, as there is no ‘smoking-gun’ evidence for either.

We claim that PAL30 is tilted for the following reasons: the smectic layer spacing is significantly less than the extended molecular length; the lower temperature phases are proven to be chiral (therefore tilted), and there is no observed smectic layer-contraction observed on cooling, which would be expected for an orthogonal \rightarrow tilted phase transition; and there is no measured change in the birefringence which would be predicted from an orthogonal phase to the <<< HEAD helical $\text{Sm}(\text{CP})_\alpha$ (confirmed from RSoXS). Though individually, none of these facts are conclusive evidence for tilt, all of them in aggregate suggest that the highest temperature smectic phase of PAL30 is tilted. ====== helical $\text{Sm}(\text{CP})_\alpha$ (confirmed from RSoXS). All of these facts together suggest that the highest temperature smectic phase of

PAL30 is tilted.

»»»> 6188fac044d2ea13f89e1169cada113c0d6ce733 To see that there is no long-range order in the tilt order parameter, we can look at the textures of this phase and observe that they look orthogonal— they have the clean lines of a focal conic SmA phase. This is necessary but not sufficient, as other phases— such as the SmC_AP_A phase – can also appear to be orthogonal, yet have a definite anti-clinic long range order. This anti-clinic order (and other, more exotic long helical ordering of «««< HEAD the tilt order parameter) would however, show up in resonant x-ray scattering. The fact ===== the tilt order parameter) would show up in resonant x-ray scattering. The fact »»»> 6188fac044d2ea13f89e1169cada113c0d6ce733 that the resonant x-ray scattering shown in ?? reveals zero periodic structure for PAL30 confirms that the tilt order in the Sm1 phase has no long-range order.

«««< HEAD The actual way that this long-range order is escaped is still ambiguous. The simplest model, ===== The actual way that this is achieved is still ambiguous. The simplest model, »»»> 6188fac044d2ea13f89e1169cada113c0d6ce733 where the molecules are rotating freely around a cone whose opening angle is set by the molecular tilt seems unlikely from simple enthalpic space-filling arguments which would seem to exclude a model where neighboring molecules can be pointing in completely opposite directions with no energy cost. On the surface, this seems to be false, but close observation of the c-director fluctuations that occur in freely-suspended-films shows that at the molecular level the c-director can easily be fluctuating with π -rotations measured against neighboring molecules, so we cannot rule out this type of behaviour purely on enthalpic concerns. This is fluid-like model, where the molecules are actively rotating with no regard for their neighbors space.

By including these enthalpic considerations we can build a model where short-range order persists, but the size of these ordered domains is small, and they are randomly distributed such that an ensemble average of the tilt is zero. This is more of a disordered-crystal model, where short-range order persists, but is distributed in such a way that the macroscopic order parameter is still zero— much like the example of a cooled Ising model developing local

need
to find
de
gennes/noel
argu-
ment
for
this

ferroelectric ordering of spins, even though the total magnetization remains zero.

Regardless of how this long-range tilt order is broken, because these are polar molecules, we also have to consider the polar-ordering present in any phase. The way that the polar and tilt interact in the high-temperature de Vries SmA of PAL30 is unique to bent-cores.

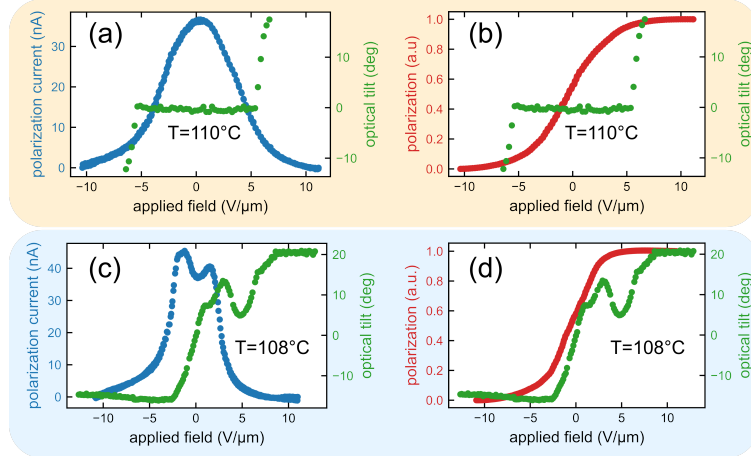


Figure 1.1: The polarization current and the optical tilt plotted as a function of applied field strength for both the Sm1 (de Vries SmA) (a,b) and the Sm2 ($\text{Sm}(\text{CP})_\alpha$) (c-d). The polarization current has additionally been integrated to calculate the time-dependant net polarization. The threshold electric field (E_{th}) required to manifest the tiger-stripes can be directly read from the green curve denoting the optical tilt (for $T=110^\circ\text{C}$, $E_{\text{th}} \approx 5 \text{ V}/\mu\text{m}$), and the saturation electric field where the net polarization is no longer changing (E_{sat}) can be directly read from the red curve, which denotes the net polarization, (for $T=110^\circ\text{C}$, $E_{\text{sat}} \approx 5 \text{ V}/\mu\text{m}$). Both E_{th} and E_{sat} are plotted in as the inset of ??.

The polarization current has been integrated to give the net polarization, which <<<< HEAD is a direct measure of the ensemble average of the molecular polar orientation with an ===== is a direct measure of the ensemble average of the molecular orientation with an >>>> 6188fac044d2ea13f89e1169cada113c0d6ce733 applied electric field. The optical tilt measurements were done by analyzing the contrast between adjacent stripes. In the ground state, where there is no long-range order present in tilt, the contrast is zero. At a field whose strength is over some threshold value (E_{th}), the state transitions into a tilted (therefore chiral) state. The handedness of the domain sets the tilt direction. This tilt can be

small
figure
show-
ing
this

directly measured as it is proportional to the contrast between different handed domains:

$$\text{contrast} \propto \sin(4\theta) \quad (1.1)$$

. Barring pathological examples, *any* alignment, orientation, or movement of the molecular long axis will show up as the observable separation of the texture into chiral domains.

check
this

With some unique exceptions[?] most bent-core systems have the tilt and polarity strongly coupled: where one moves, the other follows. Through symmetry, this can be expressed as the condition that rotations around the molecular long axis are forbidden: to transition to different states, the molecule must rotate around the smectic layer normal, confined to the tilt-cone. <<< HEAD Figure 1.1 clearly shows that for the Sm1 phase of PAL30, this is no longer the case. The movement of the polar director is completely decoupled from the movement of the c-director, which can only occur if the PAL30 molecules are rotating around the long axis, allowing their polarization to change while the optical tilt stays fixed. It is only after the polarization saturates and is completely aligned =====

cite
michi

Figure 1.1 clearly shows that the movement of the polar director (rotations around the long axis of the molecule) is decoupled from the movement of the c-director (rotations around the smectic layer normal on the tilt-cone). The polarization first saturates >>> 6188fac044d2ea13f89e1169cada113c0d6ce733 before there is any detectable movement of the tilt-director. The previous examples of this occurring in bent-cores required pulse-engineering the applied voltage, where a very large, fast voltage needed to be applied to see rotations around the long axis of the molecule. PAL30 is the first molecule where the polar <<< HEAD and tilt order are decoupled enough to allow these long-axis rotations naturally. ===== and tilt order have been confirmed to be decoupled in its ground-state. >>> 6188fac044d2ea13f89e1169cada113c0d6ce733

small
inline
figure
of this

small
inline
figure
of this

This decoupling results in an important distinction because, unlike their calamitic cousins, these bent-core molecules are not inherently chiral. They are only develop chirality once they pack into phases. they require tilt and smectic ordering before the mirror-symmetry

breaking required for chirality is achieved. They also require that the tilt and polar order are strongly coupled—free rotations around the long-axis result in a return of mirror-symmetry and the chirality of «««< HEAD the phase is lost. In contrast to the calamitics, who merely have to ‘discover’ their own inherent chirality once a field is applied (for instance, in the electroclinic effect), the bent-cores must spontaneously create their own. This is not a new discovery, the B2 phases[?] have long been known to develop spontaneous chirality on cooling from an achiral phase. This is however ===== the phase is broken. In contrast to the calamitics, who merely have to ‘discover’ their own inherent chirality once a field is applied (for instance, in the electroclinic effect), the bent-cores must spontaneously create their own. This is not a new discovery, the B2 phases[?] have long been known to develop spontaneous chirality on cooling from an achiral phase. This is »»»> 6188fac044d2ea13f89e1169cada113c0d6ce733 the first discovery of field-activated chirality in a bent-core system, where chirality is induced at a certain voltage, but then returns to an achiral ground state when the voltage is removed.

«««< HEAD The bent-core de Vries phase we discovered in PAL30 has three defining characteristics: it is tilted; it has no long-range tilt-order present, and the polarity and tilt are decoupled.

One potential approach to modelling this phase is the Landau-de Gennes =====

The closest thing to a developed model for this phase is the Landau-de Gennes »»»> 6188fac044d2ea13f89e1169cada113c0d6ce733 model put forth by Eremin et al.[?] where they discovered an electro-clinic analog in a hockey-stick compound. Broadly, their model describes an orthogonal bent-core phase where the polar director is free to move. On application of an electric-field, the polarization of the molecules orients. An enthalpicphase transition is then driven by excluded-volume interactions, where the molecules can pack more efficiently by tilting.

This interaction is described by the following Landau-de Gennes free energy:

get
and
show
the
molecule

check
this
with
ed

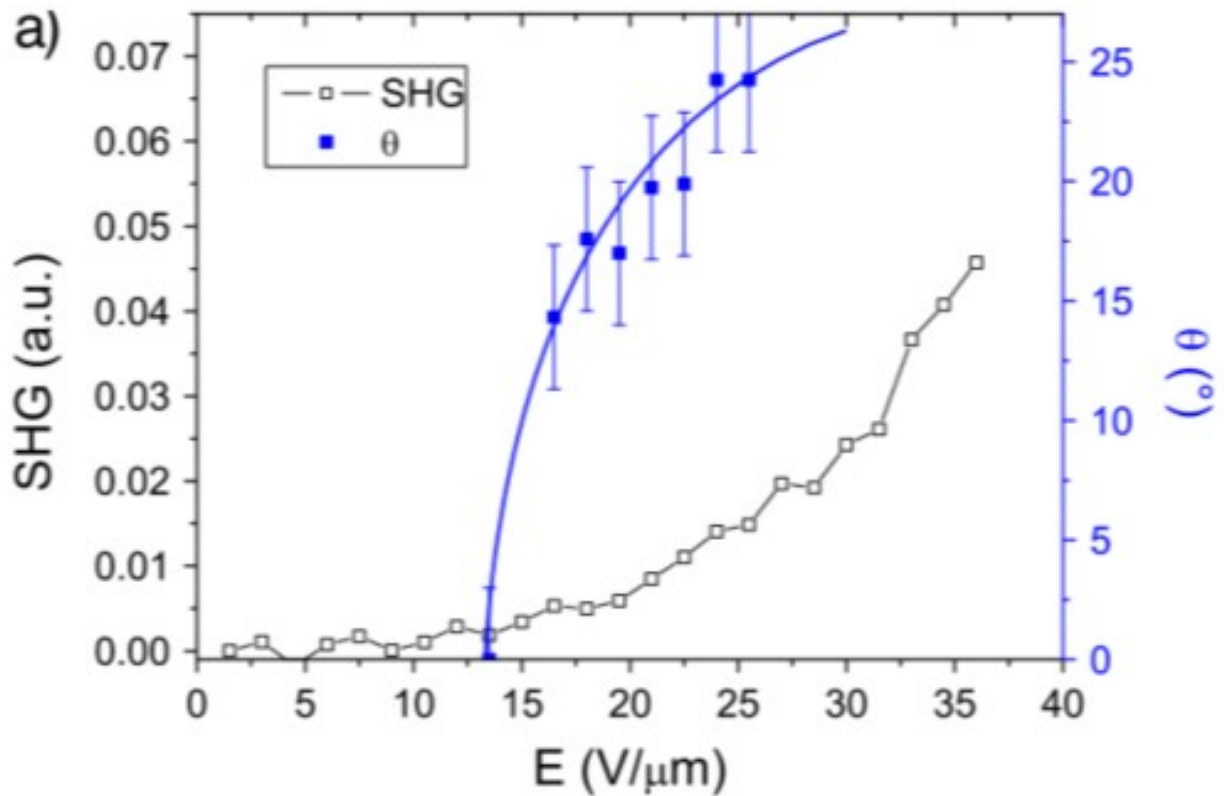


Figure 1.2: Experimental data for ‘hockey-stick’ compound studied by Eremin et al.[?] Note, the threshold for optical tilt. The lines guide the only.

$$f(P, \theta, T, E) = \overbrace{(a_0(T - T_\theta)\theta^2 + b\theta^4 + c\theta^6)}^{f_\theta} + \underbrace{(\alpha_0(T - T_P)P^2 + \beta P^4 + \gamma P^6 - PE)}_{f_P} + \underbrace{(-\Gamma(P\theta)^2)}_{f_{\theta P}} \quad (1.2)$$

Though this model was originally formulated to describe the transition from an orthogonal phase to a tilted one, we can adapt it to our bent-core de Vries phase by changing the interpretation of θ from the molecular tilt to the optical tilt.

Though this model successfully captures the overall nature of the electrically-driven onset of chirality in the bent-core de Vries phase, where the molecules first orient their polar directors to the field, and on the achievement of total polar alignment, an optical tilt develops, it leaves much to be desired. Because this model does not demand details of the microscopic interactions that lead to the observed transition, there is an abundance of fitting parameters that will lead to overfitting and the model loses most of its predictive power.

Because of this, efforts must be undertaken to develop a microscopic model of this de Vries phase.

1.2.0.1 The Beginnings of a Microscopic Model for the Bent-Core de Vries

Though the full development of this theory is beyond the scope of this thesis, I will outline the steps that must be taken.

First, the decoupling present between the polar and tilt order in the bent-core de Vries phase has to be experimentally quantified. This decoupling is realized when the molecule can rotate freely around the long axis, which can be described by a single angle, β . The other switching mode, common to conventional bent-cores, is described by a rotation around the tilt cone, described by an angle θ .

include
math
sec-
tion
show-
ing

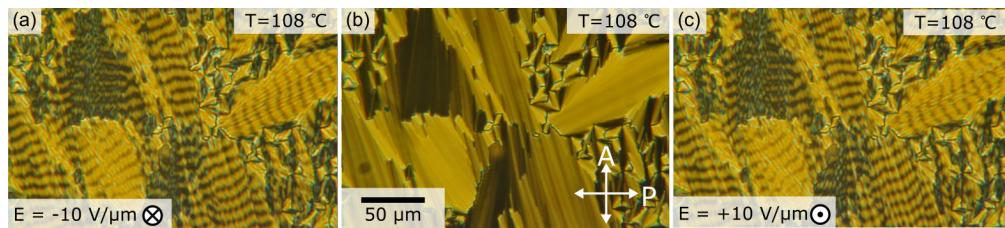


Figure 1.3:

1.2.1 Textures of bent-code de Vries phase

1.2.2 Electro-optics of bent-core de Vries phase

text text

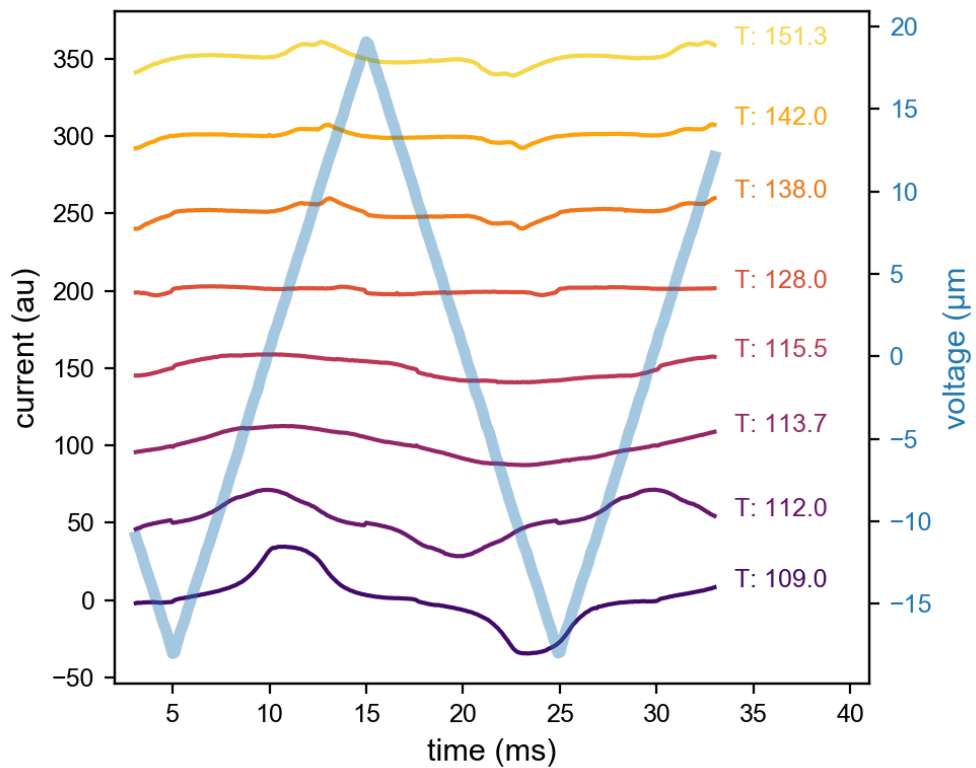


Figure 1.4:

text

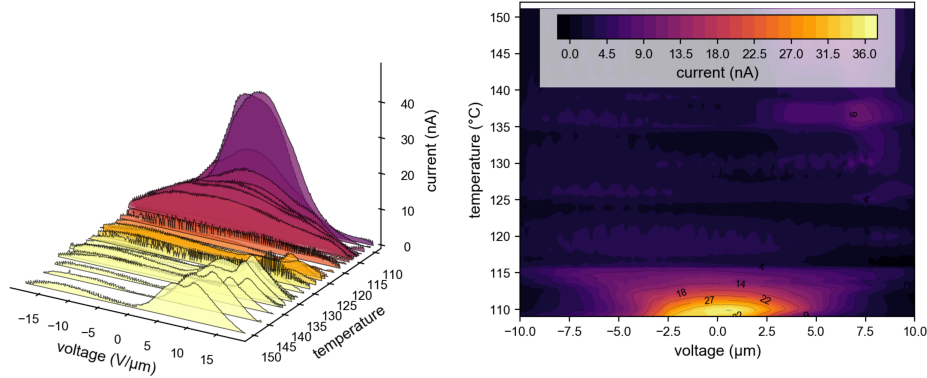


Figure 1.5:

1.2.3 X-ray analysis of bent-core de Vries phase

1.3 Discussion for the bent-core de Vries phase

1.4 Alignment-Induced Phase Transitions

It is easy to ignore that when experimentalists perform phase characterization of liquid crystals, we are not only characterizing the phase in terms of the usual statistical mechanics variables of pressure and temperature, we also must include the variable of how this material was confined. An example of this is the suppression of the long-range helix in the SmC* anti-ferro phase in thin cells. And for the majority of liquid crystal/soft matter systems, the conditions of confinement do not impact the bulk phase that dramatically, and we are right to ignore it.

However, our investigation of the homologous series of molecules related to PAL30 have revealed that the confinement conditions cannot be ignored for this series of molecules. ?? shows the same material, **n-16** in two different cells. One is an LC Vision cell, one is an Instec cell. .

The behaviour of the same material in these different cells is so different as to be a different phase. This observation goes a long way to explain why the original phase

cite
noel's
flc
stuff

need
to find
out
what
is used
for the

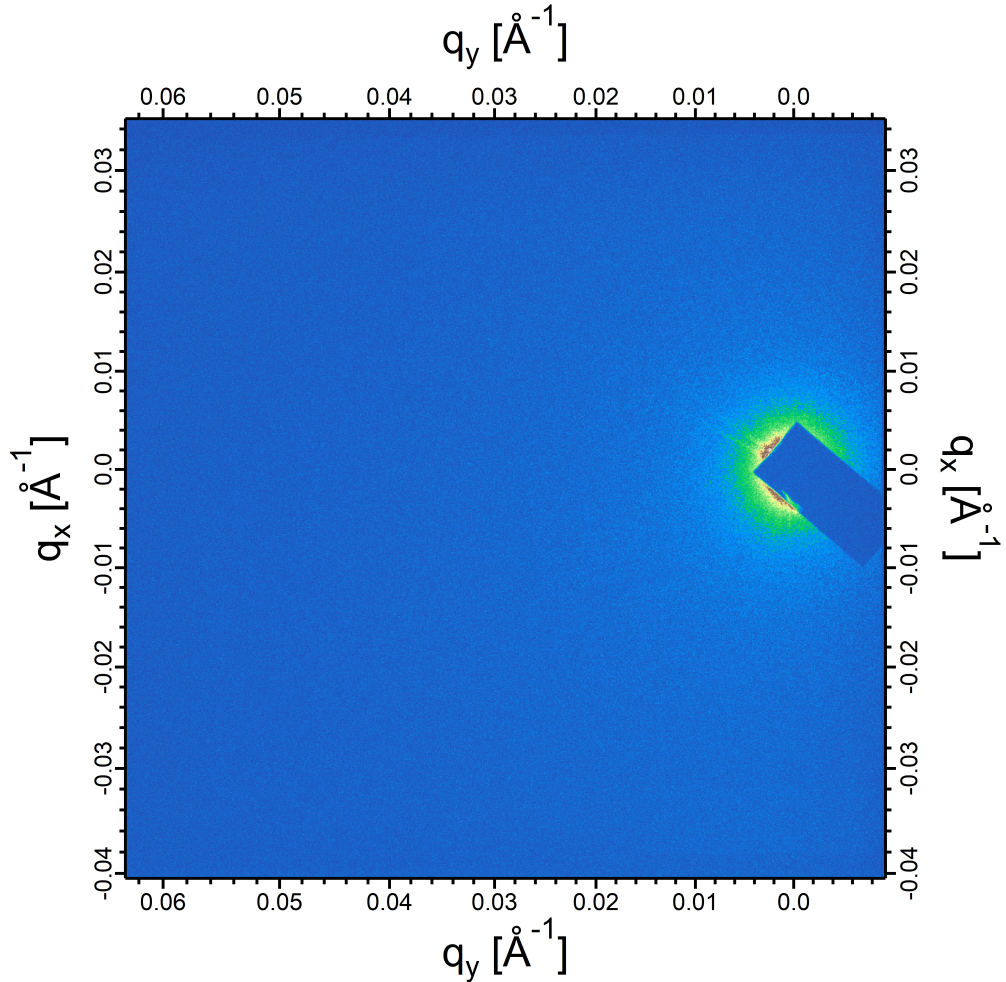


Figure 1.6:

classification of PAL30 was so contentious- it could be that the Dublin group was actually observing a different phase from our observations in Boulder.

Though we are currently limited in our ability to compare the behaviour of these materials in different cells due to a dearth of available material, we can compare the electro-optic behaviour at different temperatures.

n-16 begins switching at similar temperatures on cooling from the isotropic phase, shown in [Figure 1.9](#). In LC vision cells (which were used to characterize the PAL30 compound), the response to an applied electric field manifests as the familiar tiger stripes seen in PAL30 ([Figure 1.9 \(a-c\)](#)), with a subtle difference: while the tiger stripes seen in PAL30 were parallel

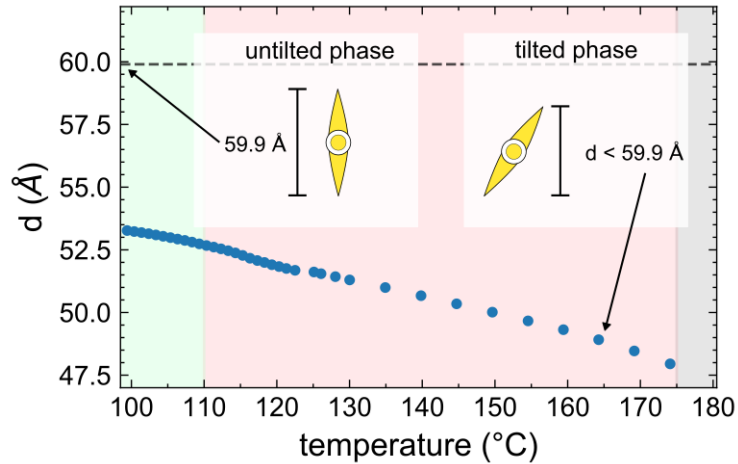


Figure 1.7:

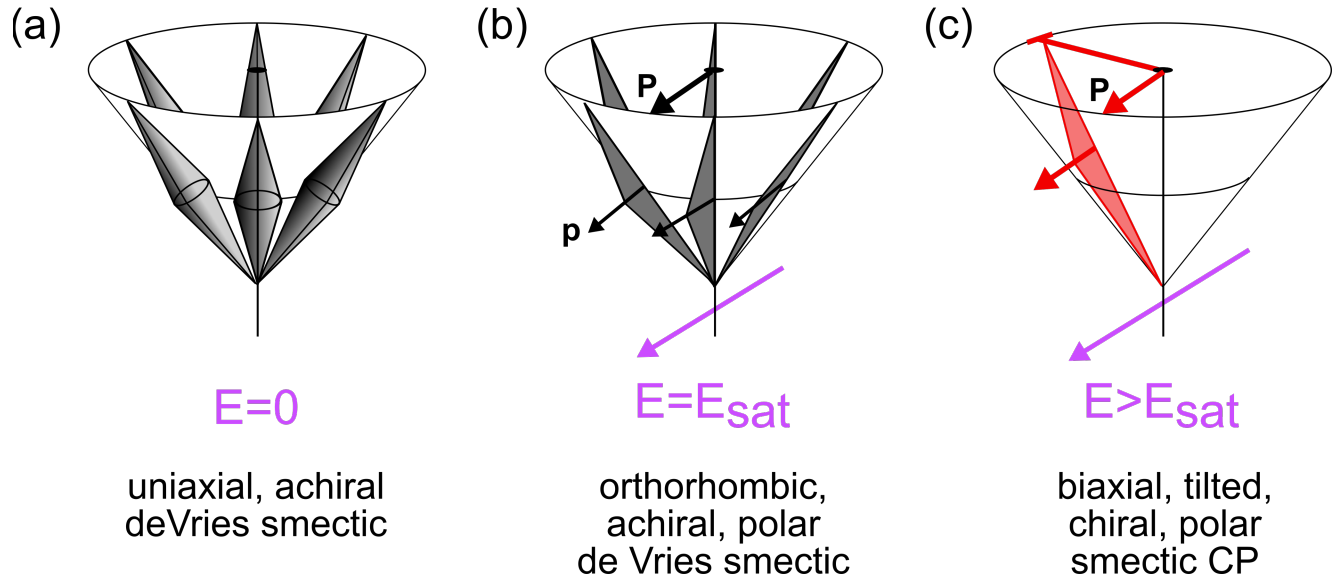


Figure 1.8:

to the smectic layers *on average*, they were wavy. The tiger-stripes seen in **n-16** are straight, indicating that they are rigidly bound to the smectic layers. The implications of this are not understood.

In the Instec cells, the response to an applied electric field manifest as a barely distinguishable change in contrast in large block-like regions (Figure 1.9(d-f)). However, these

phases look broadly similar— an orthogonal-looking ground state that switches into some chiral phase. It is only on further cooling that the texture undergo a dramatic divergence.

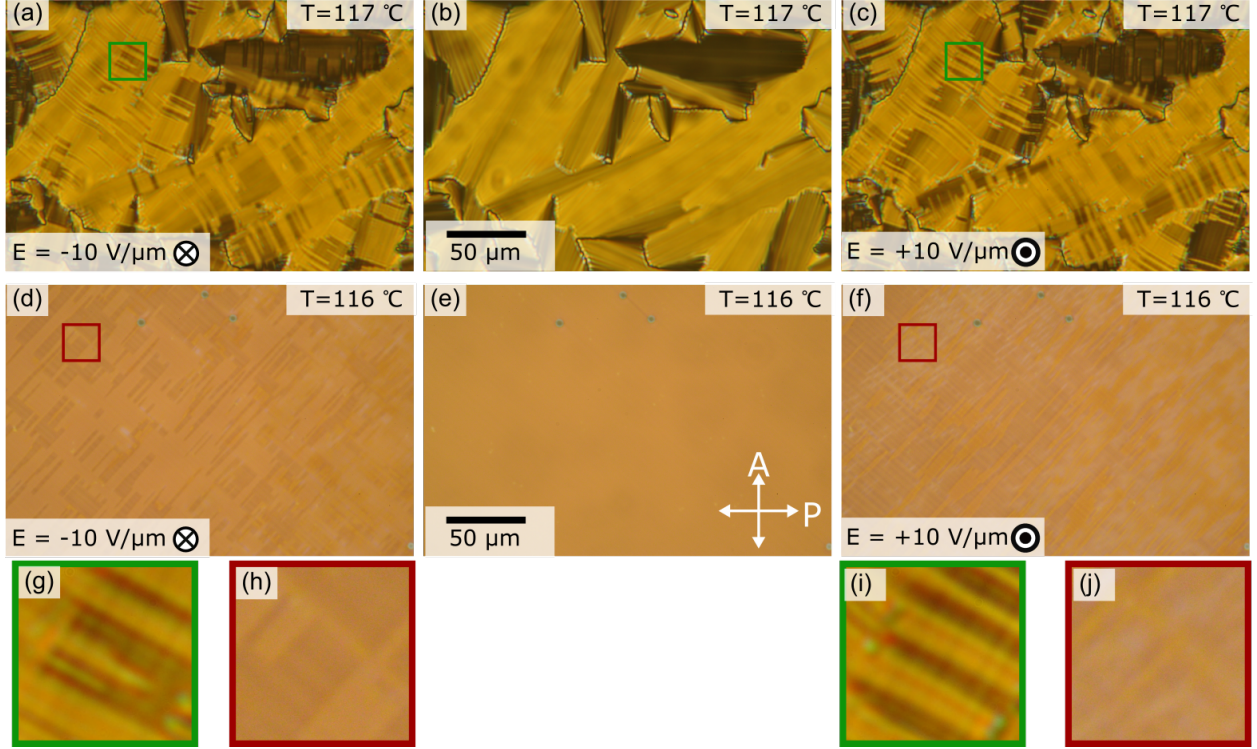


Figure 1.9: Planar textures of **n-16** at approximately 116 °C in an LC vision cell (a-c) and an Instec cell (d-f) viewed under cross polarizers. Both cells use a polyimide anti-parallel alignment layer. The LC vision cell has clear focal conics, while the Instec cell is entirely aligned. Both textures manifest chirality, seen as the distinct difference between the textures with a negative or positive out-of-plane electric field applied. The contrast between handed domains shows up clearly in the LC vision cells (compare (g) and (i)) while the contrast in the Instec cells is barely distinguishable.

Cooling to 110 °C gives a familiar SmC_AP_A like texture in the LC vision cells that looks identical to PAL30— an orthogonal like phase that switches into a clearly chiral phase, with contrast between domains of alternating chirality ([Figure 1.10 \(a-c\)](#)). However, the Instec cell appears to not be chiral— the positive and negative applied field result in a texture that appears broadly identical, indicating a mirror symmetry in the phase that precludes chirality ([Figure 1.10 \(d-f\)](#)). Instead, the birefringence increases in broad stripes that are parallel to

the smectic layers. One possible explanation is that the alignment of the bottom-plate and top-plate of the cell aligned at opposite positions on the tilt-cone. This would give a texture that could appear orthogonal, even when the polarization has been universally aligned to an external field. This is not unheard of, and one way to rule this out would be to prepare a cell with an alignment layer on only one of the plates of the cell. The other possible explanation is that the dramatic alignment caused by the Instec cell, alongwith the unique decoupling of polarity and tilt seen in these molecules, are interacting in an unforeseen way.

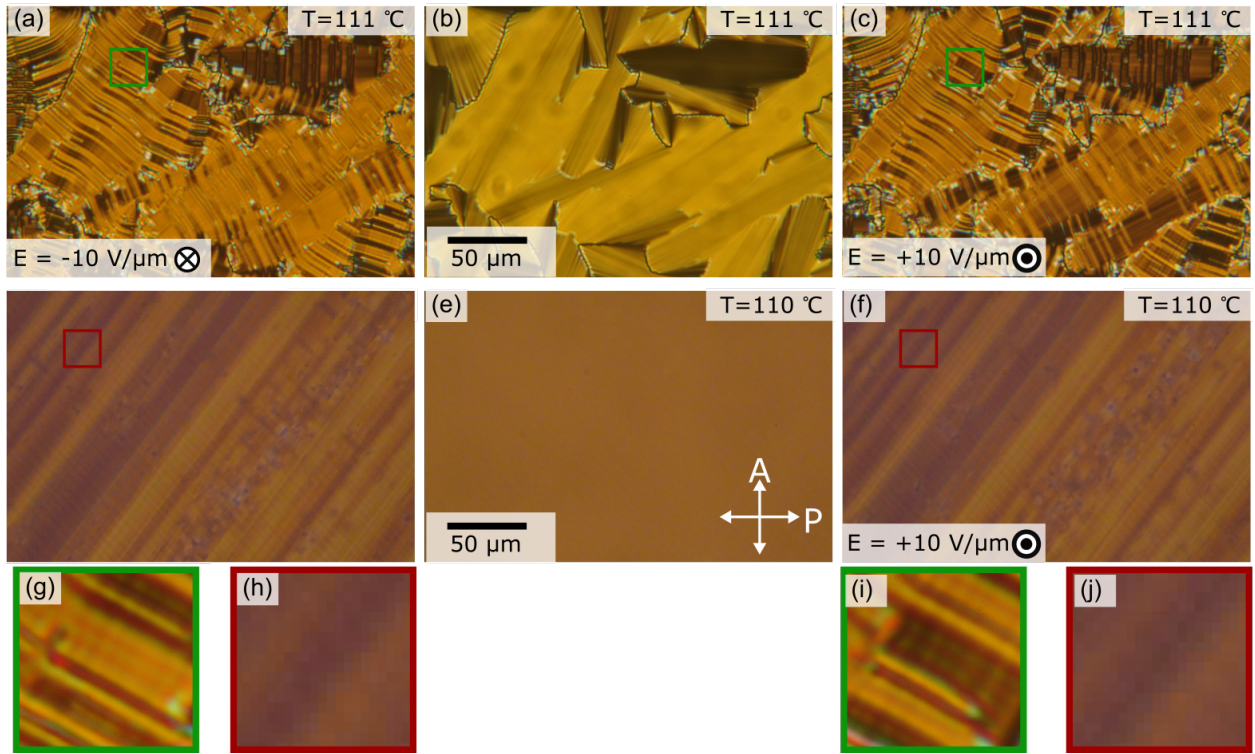


Figure 1.10: Planar textures of **n-16** at approximately 110 °C in an LC vision cell (a-c) and an Instec cell (d-f) viewed under cross polarizers. Both cells use a polyimide anti-parallel alignment layer. The LC vision cell has clear focal conics, while the Instec cell is entirely aligned. Both textures manifest chirality, seen as the distinct difference between the textures with a negative or positive out-of-plane electric field applied. The contrast between handed domains shows up clearly in the LC vision cells (compare (g) and (i)) while the contrast in the Instec cells is barely distinguishable.

Further cooling to 100 °C gives a unique texture in both the LC Vision cell, and

the Instec cell, see ???. While the PAL30 textures in this phase had regular striations of contrast present when an external field was applied, they did not manifest the riot of colour present in the **n-16** textures, where bands of different birefringences appear overlaid bands of contrast??(a-c). The cause of this is currently unknown. It is also worth noting that this state appears to be long-lived, as inspection of the texture that was previously exposed to an electric field in ?? (b), still manifest faint striations, indicating that it has not fully relaxed to an achiral ground-state.

This stands in contrast to the Instec cell, whose response under an applied electric field has actually decreases. The bands of birefringence clearly visible at 110 °C in [Figure 1.10](#) (d,f) have faded. However, the dark bands that form orthogonal to the layers (much like those caused by undulating layers in a SmA focal conic) which were only faintly visible at 110 °C in [Figure 1.10](#) (d,f) are now more pronounced.

On further cooling, the textures of both cells converge to familiar $\text{SmC}_\text{A}P_\text{F}$ switching, where the entire cell has an increase in birefringence under an applied electric field.

Solving this mystery will go a long way to advancing our understanding of how chirality develops and manifest in these soft-matter systems. We have a phase with a known chiral bulk-state (see the resonant x-ray scattering of **n-16** at 110 °C) that, in some cells (LC vision), shows its chiral nature, but in others (Instec), this chirality seems to be suppressed. The more conventional explanation, that this is still the same chiral $\text{Sm}(\text{CP})_\alpha$ phase which appears to be achiral because of some fluke in the alignment would need to first be ruled out.

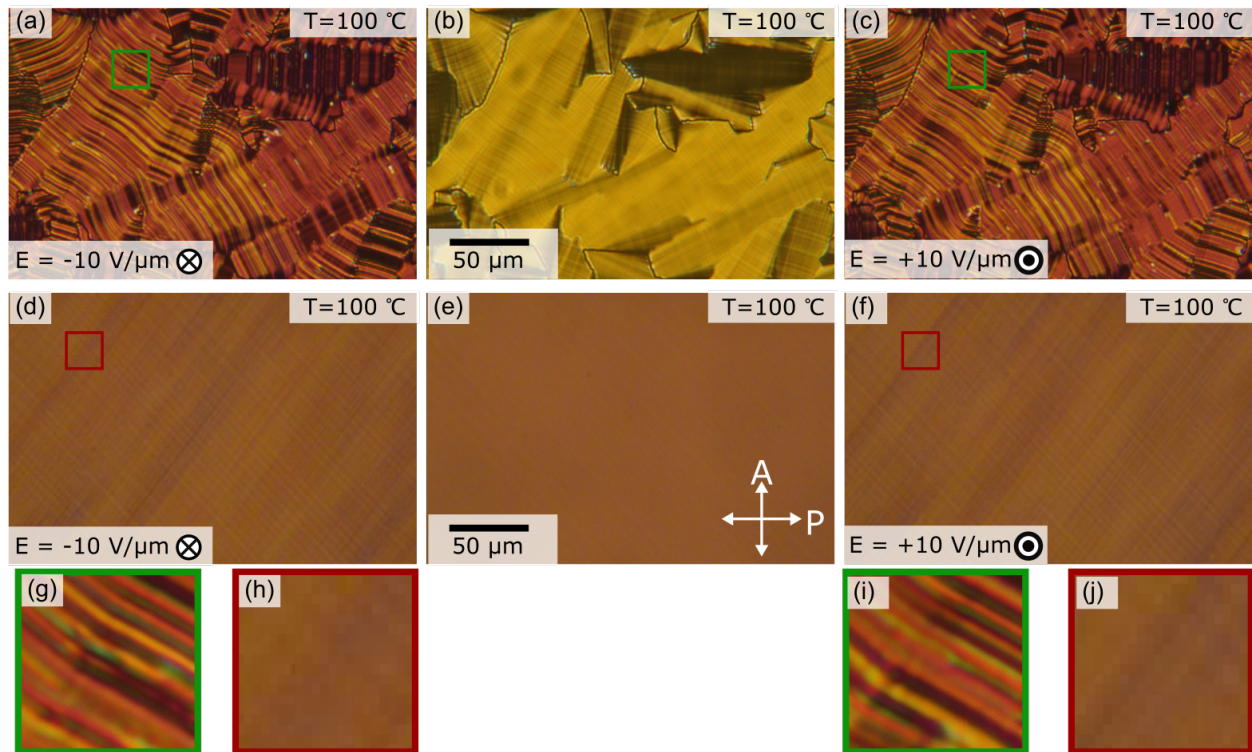


Figure 1.11: Planar textures of **n-16** at approximately 100 °C in an LC vision cell (a-c) and an Instec cell (d-f) viewed under cross polarizers. Both cells use a polyimide anti-parallel alignment layer. The LC vision cell has clear focal conics, while the Instec cell is entirely aligned. Both textures manifest chirality, seen as the distinct difference between the textures with a negative or positive out-of-plane electric field applied. The contrast between handed domains shows up clearly in the LC vision cells (compare (g) and (i)) while the contrast in the Instec cells is barely distinguishable.